s c c h
software competence center
hagenberg

FUZZY.LOGIC.LAB.LINZ

Advances in Knowledge-Based Technologies

Proceedings of the Master and PhD Seminar Summer term 2011, part 2

Softwarepark Hagenberg
SCCH, Room 0/2
15 June 2011

Software Competence Center Hagenberg
Softwarepark 21
A-4232 Hagenberg
Tel. +43 7236 3343 800
Fax +43 7236 3343 888
www.scch.at

Fuzzy Logic Laboratorium Linz
Softwarepark 21
A-4232 Hagenberg
Tel. +43 7236 3343 431
Fax +43 7236 3343 434
www.flll.jku.at

Program

Session 1. Chair: Bernhard Moser

13:00 Thomas Vetterlein:
Recent Advances in Approximate Reasoning

13:30 Edwin Lughofer:
Reliable All-Pairs Evolving Fuzzy Classifiers

Session 2. Chair: Roland Richter

14:15 Henrike Stephani:
Automatic Analysis of Terahertz Spectra

14:45 Jean-Luc Bouchot:
Characterization and Analysis of Speckle Patterns in Optical Coherence Tomography Images

Recent Advances in Approximate Reasoning

Thomas Vetterlein
Department of Knowledge-Based Mathematical Systems
Johannes Kepler University Linz
Altenbergerstraße 69, 4040 Linz, Austria
Thomas.Vetterlein@jku.at

A notion is called vague if it may happen that the objects under consideration cannot be sharply divided into those to which the notion applies and those to which it does not apply. The adjective "large", referring, for instance, to the height of trees in a forest, is an example.

Vague notions belong to a coarse level of granularity; "large", for instance, is usable only to delineate large from small objects. To reason with vague notions does not cause problems when conclusions are to be drawn on this low level of granularity. When, however, objects are considered with regard to properties involving a finer level of granularity, the coarse-level notions are usually not suitable. If their usage is nevertheless intended, they need to be interpreted within the fine level.

We present one general possibility of how to do so. Our formalism is an advancement of the Logic of Approximate Reasoning [Rus, Rod, GoRo]. The same time, it comes close to fuzzy logic in the sense of Hájek [Haj]. The disadvantage of the original version of approximate reasoning of being discontinuous under certain circumstances is removed. Moreover, the disadvantage of fuzzy logics of not having well interpretable proof systems is overcome as well.

References

[GoRo] L. Godo, R. O. Rodríguez. Logical approaches to fuzzy similarity-based reasoning: an overview, in: G. Della Riccia et al. (eds.). *Preferences and similarities*, CISM Courses and Lectures 504, Springer-Verlag, Berlin 2008; pp. 75 - 128.

[Rod] R. O. Rodríguez. *Aspectos formales en el Razonamiento basado en Relaciones de Similitud Borrosas, Ph. D. Thesis*, Technical University of Catalonia (UPC), 2002.

[Rus] E. Ruspini. On the semantics of fuzzy logic, *International Journal of Approximate Reasoning* **5** (1991), 45 - 88.

[Haj] P. Hájek. *Metamathematics of fuzzy logic*, Kluwer Academic Publishers, Dordrecht 1998.

Reliable All-Pairs Evolving Fuzzy Classifiers

Edwin Lughofer[1]

Abstract

In this paper, we propose a novel design of evolving fuzzy classifiers (EFC) *for multi-class classification problems. Therefore, we exploit the concept of all-pairs (AP) aka all-versus-all classification using binary classifiers for each pair of classes. This benefits from less complex decision boundaries to be learned opposed to direct multi-class approach as well as achieves a higher efficiency in terms of incremental training time than one-versus-rest classification techniques. Regression-based as well as singleton class label fuzzy classifiers are used as architectures for the binary classifiers, which are evolved and incrementally trained in a data-streaming context. The classification phase considers the preference levels of each pair of classes collected in a preference relation matrix and uses a weighted voting scheme on this matrix by taking into account the reliability of the binary classifiers as integrating the degree of ignorance of samples to be classified. Furthermore, the concept of conflict is handled appropriately in form of conflict models in the single binary classifiers as well as when calculating the final class response based on the preference relation matrix. The advantage of the new evolving fuzzy classifier concept over single model (using direct multi-class classification concept) and multi model (using one-versus-rest classification concept) architectures will be underlined by empirical evaluations and comparisons at the end of the paper based on high-dimensional real-world multi-class classification problems.*

Index Terms

evolving fuzzy classifiers, multi-class classification, all-pairs classification, incremental learning, preference level, preference relation matrix, reliability, ignorance, conflict

Edwin Lughofer[1] is with the Department of Knowledge-based Mathematical Systems, Johannes Kepler University of Linz, Austria, email: edwin.lughofer@jku.at

Automatic Analysis of Terahertz Spectra

Henrike Stephani

henrike.stephani@itwm.fraunhofer.de

Abstract

The technology of Terahertz time-domain spectroscopy (THz-TDS) is used here to classify measurements by their characteristic peaks in the spectrum. From the data acquisition to the classification the goal is to achieve a high level of automation and standardization and at the same time preserve adaptability.

Several steps to achieve that will be introduced. We will start by presenting various preprocessing possibilities that should be applied to enhance the quality of the spectra. After the measurements are transformed into a well interpretable form they have to be organized automatically. For this purpose we use unsupervised classification. Because it does not need input parameters to produce a result, we use hierarchical clustering. The classical version of which is easily implemented and can be adapted to the respective application by choosing the right distance measures. To handle high volume data, an algorithm that uses pre-clustering is used. To be able to evaluate the result of an unsupervised classification we furthermore propose a new evaluation scheme.

Because the input data is very high-dimensional in its features, methods that reduce that dimensionality have to be applied. Furthermore these methods have to be evaluated. To be able to perform such an evaluation we propose a simulation scheme that produces spectra which resemble THz-TDS spectra in shape, noise characteristics, and peaks. Thereby we can produce spectra with a known ground truth and use them for evaluation.

The feature reduction is then performed by only using wavelet coefficients of a certain scale. Although this seems to produce already good results wavelet coefficients have two major disadvantages: they are not shift invariant and their height does not necessarily represent the height of the original time-series. Therefore, we propose to alternatively use so-called complex wavelets. Though the number of coefficients on one level is thereby increased by a factor of two, the transform is shift invariant and improves the interpretability of the singularities by a direct representation of shifts in the phase and height in the magnitude coefficients. These feature sets are evaluated with the evaluation scheme and a correlation analysis.

Further work will consists in evaluating the features by the proposed cluster evaluation scheme and showing various real-world application examples.

Technical Report
FLLL–TR–1103

FUZZY.LOGIC.LAB.LINZ

Characterization and Analysis of Speckle Patterns in Optical Coherence Tomography Images

June 14, 2011

Jean-Luc Bouchot
Fuzzy Logic Laboratorium Linz
email: jean-luc.bouchot@jku.at

Abstract — In this talk we are interested in analyzing speckle patterns in OCT scans of a polymer material being stressed. Some special care should be taken in order to assess the displacements or the dynamics of the speckles as the images have particular characteristics: heavy noise, low signal-to-noise ratio, low structural information.

We will present some new low-level image correlation methods which allow a local characterization of the speckle patterns by means of displacement fields or local dynamic characterization. We will also present some ideas for post-processing these characterizations for segmentation purposes.

Key words — *Optical Coherence Tomography, Low-level correlation, flow-field, optical flow, clustering*

Institut für Wissensbasierte Mathematische Systeme
Johannes Kepler Universität Linz
Altenberger Str. 69
A-4040 Linz
Austria

Fuzzy Logic Laboratorium Linz
softwarepark hagenberg
Softwarepark 21
A-4232 Hagenberg
Austria

1 Introduction

Optical Coherence Tomography (OCT) is an imaging technique which allows to get information from the subsurface area of a material. We are interested here in analyzing the internal behavior of a polymer tissue being stressed.

The problem of analyzing speckled images is challenging. They are characterized by their high sensitivity to noise, as well as they rather low amount of structural information. In these cases, it is impossible to track the displacements by traditional methods and any feature-based matching would fail. Motivated by the first results obtained in [14], we extended the algorithm from a charcterization of the dynamics to the computation of flow fields by local low-level correlation techniques.

The talk is articulated as follows. In the next section we give some hints on how the images are obtained and what are their characteristics. Then, in Section 3 we describe our approaches for local analysis of speckles dynamics. The following section is dedicated to the experiments and Section 5 gives some ideas on how to make use of the results of the previous sections in order to segment an image into 3 main areas: static parts (where the internal structures stay almost the same), dynamic parts (where a flow field computation makes sense) and a noisy part (where the information carried by the speckles is corrupted by noise).

2 OCT Image: Acquisition and Characteristics

OCT imaging is a rather novel imaging process [11] for subsurface investigation of tissue. It is often used in a medical context for analysis of the retina [3] or for skin analysis purposes [4]. It has recently been adapted for material sciences and non desctructive testing [13] in the context of polymer being stressed [14]. The challenge is now to find some digital image processing techniques for its automatic exploitation.

We first describe the acquisition set up in the following subsection and then give some ideas of the challenging problems related to OCT images in Subsection 2.2.

2.1 Set-up

OCT images are based on low-coherence interferometry of (typically) near infra-red light. It can achive sub-millimeter accuracy with deeper penetration as confocal microscopy in scattering tissues. The images are acquired by a CCD camera at the output of an interferometer; see Fig 1.

A light source is splitted into 2 beams through a beam splitter. The first one will act as the reference beam while the second one will be diffracted in the scatterers of the samples. Finally, both beams are merged again together interferring with one another. These intereference patterns convey information on how much structure in the sample send back light. By analyzing these structures we can, as we will show in the next Sections, characterize the internal modifications of the material.

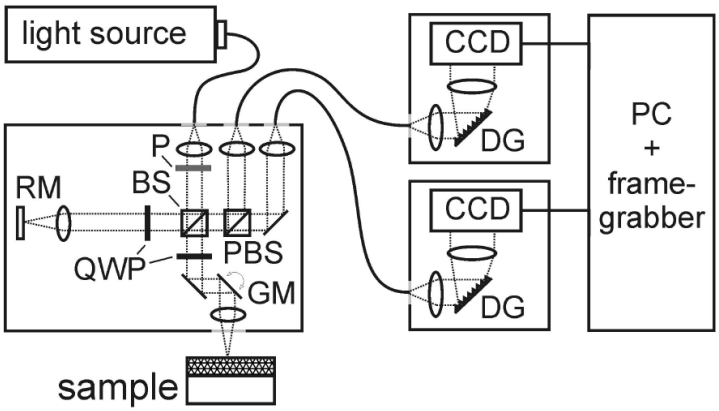

Figure 1: Sketch of the setup for the acquisition of the OCT images; reference mirror (RM), polarizer (P), beamsplitter (BS), polarizing BS (PBS), quarter wave plates (QWP), galvano-scanner mirror (GM), diffraction gratings (DG), line camera (CCD).

2.2 Characteristics

The images obtained with the presented setup are completely different than any images taken with a camera of a natural scene; see Fig. 2 for an illustration. The contrast is high only due to the presence of speckles and the (interesting) structural aspects are rather on low-contrast area. Moreover, it must be known that these OCT images are corrupted by speckle noise. One can distinguish two types of speckles. The first one is a complete random noise created by multiple backscattering in the sample, which we call the signal degrading speckles. The second one is the one of importance and comes from the scattering in the focal plane of the lenses. It is denoted as signal carrying speckles.

This particularity of speckles in OCT images as being both signal degrading and signal carrying makes it hard to analyze the images. Indeed one cannot only filter out the speckles and work on the resulting image, as it would leads to a lack of information, and therefore more adequate techniques should be develop, as we will see in the next section.

3 Local Analysis of Speckled OCT

In this section we present our main contributions to this talk. As stated in the previous section, processing speckled images is challenging as noise appear as signal carrying as well as proper noise. These problems have already been stated in [14] together with some first ideas for the processing of such images.

Here we are interested in improving the interpretation of OCT obtained speckled images. We have developped different methods for the characterization of the dynamics of the speckles. We give details of the two main classes of appraoches: local dissimilarity measures and local correlations.

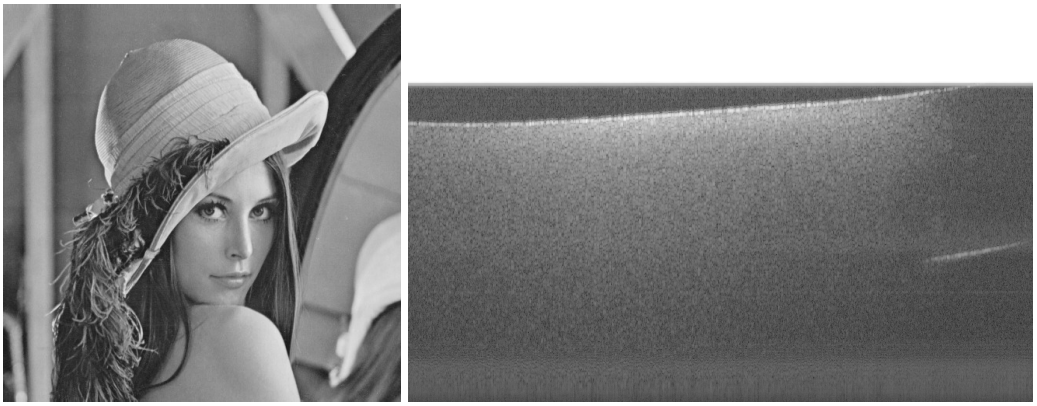

(a) Example of a grayscale natural image (b) Example of an OCT scan of a polymer material

Figure 2: Some examples of natural image scenes and OCT speckled images. It appears clearly that the structural aspects of the material are within low-contrast area of the OCT scan.

3.1 Local Dissimilarity Measures

This method was first introduced in [14] and deeper analyzed in [5]. It allows us to clearly separate dynamic region of a material from more static ones. It is based on the work of Baudrier *et al.* [1] on the topic of binary image comparison. The authors computed a so called *Local-Dissimilarity Map (LDMap)* based on the Hausdorff distance. Another work is done to assess the quality of a Magnetic Resonnance Image (MRI) [10]. We adapted this approach to compare two images within a time shift. We adapted this method to be capable of different metrics. The *LDMap* considers a small neighborhood centered at a given pixel of a given frame and computes the dissimilarity with the same neighborhood from the consecutive frame. The *LDMap* computation is done as follows:

$$\forall 1 \leq i \leq M,\ \forall 1 \leq j \leq N, \text{LDMap}[d](i,j) = d(I^{(t)} \circ A(i,j), I^{(t+1)} \circ A(i,j)) \tag{1}$$

with M, N being the size of the input images, $A(i,j)$ a windowing function around pixel (i,j). t is an index corresponding to the time.

It was empirically verified that the local dissimilarity gives a good idea of the dynamics of the speckles from the tested materials.

Parameters As it appears in Eq. 1 defining the LDMap two major parameters should be taken into account and tuned depending on the applications.

The most important one seems to be the choice of the **window size**. Indeed taking a bigger size for the window will increase the risk of averaging out the speckles present. As we stated in the theory in Sec. 2 we should not get rid of the local speckles as they are responsible for conveying the signal information. On the other hand, by taking a too small windowing function we will not get any robust estimation of the disparities. Indeed if we assume an extreme case as being the one where we consider the windowing function as a single pixel (i,j) itself, the dissimilarity computation will return an almost binary values which can be interpreted as follows: *is the speckle still at the same place or not?* Practical results will be shown in the experimental part, Sec. 4, Fig. 4(a) to Fig. 4(c). They show that the *LDMap* is a good indicator of the presence of noise or displacements.

A second parameter is the choice of the **dissimilarity measure** d. In the experiments we have made on polymer materials (see details in Sec 4.2), it seems that this parameter as much less impact than the previous one. In our tests ye did not remark some main differences after changing this parameter and we will threefore keep on with the classical euclidean norm.

3.2 Local Correlation Methods

The methods we present here aim at describing quantitatively the speckles displacements. Each of presented methods yield an image of 2 dimensional vectors containing the optimal x displacement on one side and the y one on the other.

Here again the different methods can be classified into two categories: the pixel based methods, and the frequency based ones.

3.2.1 Local Cross Correlation

In this approach we define a speckled window as being part of a neighboring region. The aim is to find in the neighboring region inside the consecutive images where we are more likely to find the given speckled window.

Correlation The correlation coefficient used is the one defined by Lewis [7]. It is defined, for a given input window w, on a neighborhood $\mathcal{N}$ as

$$NCC(u,v) = \frac{\sum_{(x,y)\in w}\left(\mathcal{N}(x-u,y-v) - \overline{\mathcal{N}}_{u,v}\right)\left(w(x,y)-\overline{w}\right)}{\{\sum_{(x,y)\in w}\left(\mathcal{N}(x-u,y-v) - \overline{\mathcal{N}}_{u,v}\right)^2 \sum_{(x,y)\in w}\left(w(x,y)-\overline{w}\right)^2\}^{\frac{1}{2}}} \quad (2)$$

where the overbar denotes the average, eventually centered at location (u,v). Finding the correlation peak for each patch gives us a u and v for the displacements of the window.

The whole process works as follows:

- Define window and neighborhood sizes
- For all window in img1, look for highest correlation in img2 on neighborhood. The position of the peak in the correlation tells us the local displacement.

Parameters Of course here again there are two main parameters to be tuned. The first one is here again the size of the **windowing**. For the same reasons as earlier, this is a crucial that one has to tune well. The other is this time the size of the neighborhood considered for the search. Indeed, as the speckles have some kind of randomness, the choice of a large neighboring search will increase the chance to find more than only one really similar region and therefore could lead to misinterpretation of the results or non unicity of the solution. In this case, which correlated solution should be the good one?

Fig. 4(d) to 4(f) show some examples of results of local cross correlation with different windowing size.

3.2.2 Optical Flow

Optical flow is another technique coming from a completely different area. It has been used in computer vision for instance for the purpose of image compression [8] or tracking [6, 12]. However as the aim of the optical flow is to keep track of some information within a time delay it motivates us to use this approach for speckle tracking. Many algorithms have been developped in the past years and while numerous papers can be found on the topic, we refer the reader to [15] for a good and recent description of the method.

Basically, the aim of optical flow is to minimize the following objective function:

$$\begin{aligned} E[I^{(t)}, I^{(t+1)}](\mathbf{u}, \mathbf{v}) = \sum_{i,j} \{ & \rho_D \left(I^{(t)}(i,j) - I^{(t+1)}(i + u_{i,j}, j + v_{i,j}) \right) \\ & + \lambda(\rho_S(u_{i,j} - u_{i+1,j}) + \rho_S(u_{i,j} - u_{i,j+1}) \\ & + \rho_S(v_{i,j} - v_{i+1,j}) + \rho_S(v_{i,j} - v_{i,j+1}))\} \end{aligned} \tag{3}$$

where **u** denotes the horizontal displacement field, **v** the vertical one, and ρ_D and ρ_S are respectively the data and spatial penalty functions. λ is a regularitzation parameter. Remark that the first term in the sum can easily be understood as a pattern matching (find the best match) whereas the second one ensures a given smoothness on the flow-field: close pixel should mainly have close flow.

An application of the optical flow to the speckle pattern analysis is illustrated on Fig. 3(c).

The three above described methods are all part of the pixel-based methods. The following ones are based on a frequency analysis.

3.2.3 Phase-correlation

The main idea here is to use the property of the Fourier transform to recover the displacement, consider as a translation of a pattern.

If we denote by $\mathcal{F}$ the 2 dimensional fourier transform and by δ_x and δ_y the displacements in x and y direction respectively, the following holds:

$$\mathcal{F}\left(f(\cdot - \delta_x, \cdot - \delta_y)\right)(\mu, \nu) = e^{-j(\mu\delta_x + \nu\delta_y)} \mathcal{F}(f)(\mu, \nu) \tag{4}$$

Therefore any shift in the spatial domain is converted into a shift in the phase of the fourier transform. Therefore, we are looking for a peak of the correlation function in the frequency domain instead of the peak in the space domain.

The results obtained on some artificial dataset are shown in Fig. 4(g) to 4(i). They show the importance of having a rather large area for a better estimation of the displacements in the Fourier domain.

3.2.4 Pseudo Stokes Vector Correlation

This idea is based on the work of Wang *et al.* [16]. Before computing the local correlations, it transforms an image (and its consecutive one) in a complex representation using the Riesz transform. It allows, after a local linear approximation, to compute at each pixel a 3 dimensional vector: the Pseudo Stokes Vector.

Once the three components per pixel are obtained, the correlation is done by averaging a combination of the correlation of the three components independently:

$$PSVC_{corr}(I_1, I_2) = \mathcal{C}(S_1(I_1) \times S_1(I_2), S_2(I_1) \times S_2(I_2), S_3(I_1) \times S_3(I_2)) \quad (5)$$

where $\mathcal{C}$ denotes the chosen combination of correlations.

As for the phase-correlation or the normalized cross correlation, we try to find the peak of the correlation of a patch of the first image in a neighborhood of the second image.

Parameters There are different parameters to be tuned depending on the applications and the aspect of the image. As always the choice the **w**indow size which defines the local domain used for the correlation is important. As already stated in [16], the biggest the averaging size, the more robust the approach is. This effect can be seen on Fig. 4(j) to 4(l). While it seems that taking a too big averaging window would yield bad results (as seen on the last figure), one should notive that we encounter some strong border effects when considering a 23×23 averaging on a 50×50 image.

4 Experiments

In order to assess the quality of the methods we have carried tests on two dataset. The first one being an artificial dataset shows the feasibility of our methods whereas the second one shows the complications inherent to real-world examples.

4.1 Artificial Dataset

For evaluation purposes we have designed some test samples were we can control the noise added to the images, and the part of images being either dynamic, static or noisy, as it is the case when dealing with real samples. Such toy examples can be seen on 3, where the left image represent the original one and the following one is created by shifting the left part to the bottom by a given values (in this case 3 pixels). The whole image is corrupted by speckle noise with different variances.

These images have been analyzed with the different methods presented in the previous section with their parameters varying. The results can be seen in Fig. 4.

4.2 Polymer Samples

Some real world examples taken from some tests of material testing on polzmer were used. Some samples are given in Fig. 5. For space reasons we will show only the results obtained with the LDMap and phase correlation. We decided to stick at those ones, as they are the ones which show the more robust results within fine tuning of the parameters. All the other methods (except from the optical flow) indeed need to be carefully addapted to each casem and for comparable results. The optical flow appears to be a rather unreliable method whenever it comes to real-world examples.

The most interesting figure (Fig. 5(d)) shows some distincts regions. The white one represents the parts of the material where the structure stays static along time. On the left side, one sees some

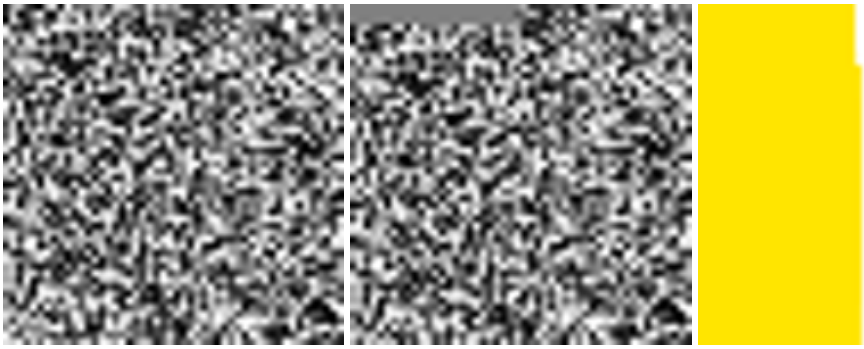

(a) Original Image (b) Distorded Image (c) Optical Flow

Figure 3: An artificial OCT scan created by adding random speckle noise to a uniform pattern. The distorded image is obtained by shifting half of the image to the bottom. Both images are 50×50 pixels large. The third image shows their optical flow.

more dense pink region which is the part of the material where the scaterrers are fleeing. The rest of the image contains some high speckle noise, which makes either unusable or unusefull. The aim of the next Section is to give some idea on how to make use of such flow in order to automatically separated each area.

5 Segmentation

As we are aiming at segmenting an image into 3 major regions: dynamic region, static region, and noisy one, we want to apply some unsupervised clustering to the results given by the computations described in Section 3. This Section aims at giving the first ideas developed for this purposes, even if the work is still under development.

5.1 Features

First of all, we want to characterize grossly how the three regions are, visually, distinct. We should note that the dynamic region are characterized by rather smooth and consistent displacement fields, which means that the different flow on a local neighborrhod should not have many disparities. A static region is characterized by low dissimilarity from an image to the following one. Finally the noisy region will both have high displacements and unconsistent directions in the displacement fields. These ideas are summarized in Table 1 in terms of local dissimilarity, gradient magnitude and entropy of weighted histograms (see for instance [2] for some information).

5.2 Spectral Clustreing

Spectral clustering is a method developed for unsupervised classification based on spectral transformations of an affinity matrix. As this part of the work is still in progress, and because no particular work has been done on the process, we refer the reader to the work of Luxburg [9] for a relevant introduction on the topic.

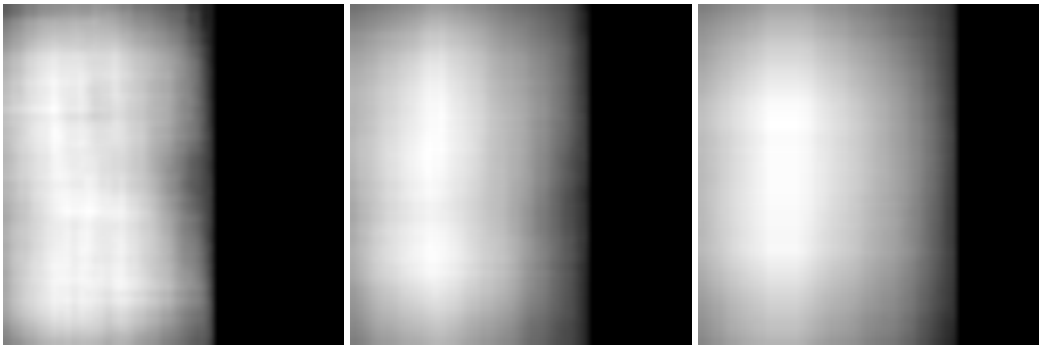

(a) LDMap obtained on a 14×14 neighborhood (b) LDMap obtained on a 22×22 neighborhood (c) LDMap obtained on a 28×28 neighborhood

(d) NCC obtained on a 3×3 neighborhood (e) NCC obtained on a 7×7 neighborhood (f) NCC obtained on a 9×9 neighborhood

(g) Phase correlation obtained on a 7×7 neighborhood (h) Phase correlation obtained on a 11×11 neighborhood (i) Phase correlation obtained on a 15×15 neighborhood

(j) PSVC obtained on a 11×11 neighborhood (k) PSVC obtained on a 19×19 neighborhood (l) PSVC obtained on a 23×23 neighborhood

Figure 4: Results for the dynamic estimation of speckles using different methods and parameters

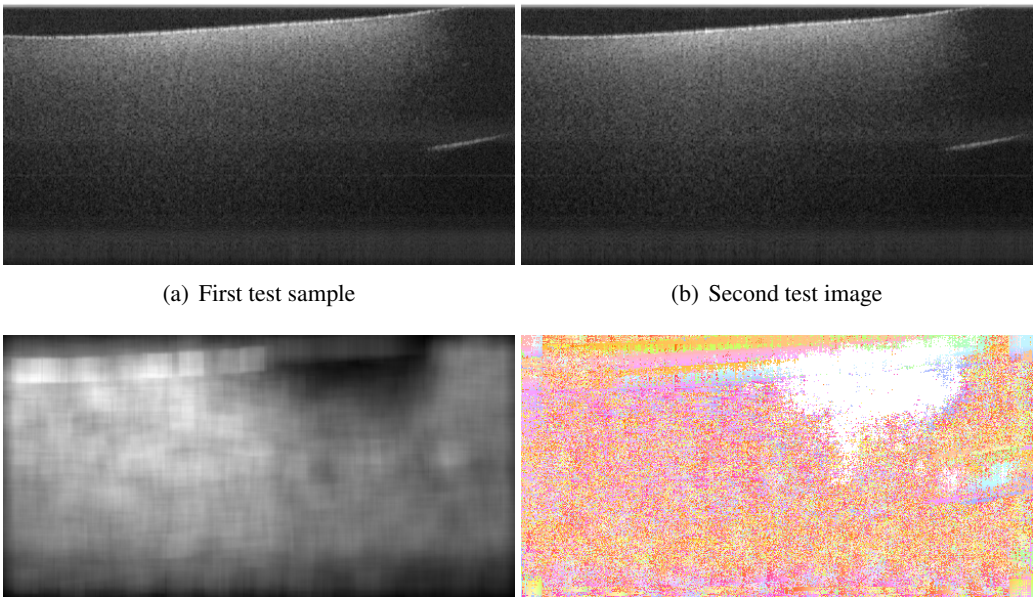

(a) First test sample (b) Second test image

(c) LDMap. window: 24×24 (d) Local Phase Correlation. Window: 21×21

Figure 5: Results on some real-world examples, using the LDMap and the phase based correlation.

Table 1: Interest of the chosen feature for the task of separating the three different region in our OCT images

	Flow Magnitude	Entropy of Directions	Dissimilarity
Static	Low	High	Low
Dynamic	High	Low	High
Noise	High	High	High

6 Conclusion

We have presented some methods for the analysis of speckled patterns in OCT scans. While the first results are promising some work is still undergoing for the post processing of the flow fields obtained. Moreover, a subpixel accuracy module should be embedded to give more robust results. This would allow indeed to work with faster setup and therefore get accurate results.

On the other hand, in the context of non-destructive material testing, we are interested in classifying the images into distinct region. Therefore the classification module should be adapted carefully and the features given should be studied deeper in the near future.

References

[1] BAUDRIER, E., MORAIN-NICOLIER, F., MILLON, G., AND RUAN, S. Binary-image comparison with local-dissimilarity quantification. *Pattern Recognition 41*, 5 (May 2008), 1461–1478.

[2] DALAL, N., AND TRIGGS, B. Histograms of oriented gradients for human detection. In *International Conference on Computer Vision & Pattern Recognition* (INRIA Rhône-Alpes, ZIRST-655, av. de l'Europe, Montbonnot-38334, June 2005), C. Schmid, S. Soatto, and C. Tomasi, Eds., vol. 2, pp. 886–893.

[3] GÖTZINGER, E., PIRCHER, M., AND HITZENBERGER, C. K. High speed spectral domain polarization sensitive optical coherence tomography of the human retina. *Opt. Express 13*, 25 (Dec 2005), 10217–10229.

[4] KORDE, V. R., BONNEMA, G. T., XU, W., KRISHNAMURTHY, C., RANGER-MOORE, J., SABODA, K., SLAYTON, L. D., SALASCHE, S. J., WARNEKE, J. A., AND ALBERTS, D. S. Using optical coherence tomography to evaluate skin sun damage and precancer. *Lasers in surgery and medicine 39*, 9 (2007), 687 – 695.

[5] LEISS-HOLZINGER, E., CAKMAK, U. D., HEISE, B., BOUCHOT, J.-L., KLEMENT, E. P., LEITNER, M., STIFTER, D., AND MAJOR, Z. Evaluation of structural change and local strain distribution in polymers comparatively imaged by ffsa and oct techniques. submitted to Express Polymer Letters, June 2011.

[6] LEPETIT, V., AND FUA, P. Monocular Model-Based 3D Tracking of Rigid Objects: A Survey. *Foundations and Trends in Computer Graphics and Vision 1*, 1 (2005), 1–89.

[7] LEWIS, J. P. Fast normalized cross-correlation. In *Vision Interface* (1995), Canadian Image Processing and Pattern Recognition Society, pp. 120–123.

[8] LIN, S., SHI, Y. Q., AND ZHANG, Y.-Q. An optical flow based motion compensation algorithm for very low bit-rate video coding. In *Acoustics, Speech, and Signal Processing, 1997. ICASSP-97., 1997 IEEE International Conference on* (apr 1997), vol. 4, pp. 2869 – 2872 vol.4.

[9] LUXBURG, U. A tutorial on spectral clustering. *Statistics and Computing 17* (December 2007), 395–416.

[10] MORAIN-NICOLIER, F., LANDRÉ, J., AND RUAN, S. Gray level local dissimilarity map and global dissimilarity index for quality of medical images. In *7th IFAC Symposium on Modelling and Control in Biomedical Systems* (Aalborg, Denmark, Aug. 2009), pp. 281–286.

[11] SCHMITT, J. Optical coherence tomography (oct): a review. *Selected Topics in Quantum Electronics, IEEE Journal of 5*, 4 (jul/aug 1999), 1205 –1215.

[12] SHIN, J., KIM, S., KANG, S., LEE, S.-W., PAIK, J., ABIDI, B., AND ABIDI, M. Optical flow-based real-time object tracking using non-prior training active feature model. *Real-Time Imaging 11* (June 2005), 204–218.

[13] STIFTER, D. Beyond biomedicine: a review of alternative applications and developments for optical coherence tomography. *Applied Physics B: Lasers and Optics 88* (2007), 337–357. 10.1007/s00340-007-2743-2.

[14] STIFTER, D., LEISS-HOLZINGER, E., HEISE, B., BOUCHOT, J.-L., MAJOR, Z., PIRCHER, M., GÖTZINGER, E., BAUMANN, B., AND HITZENBERGER, C. K. Spectral domain polarization sensitive optical coherence tomography at 1.55 mu m: novel developments and applications for dynamic studies in materials science. In *Optical Coherence Tomography and Coherence Domain Optical Methods in Biomedicine XV* (Jan. 2011), J. G. Fujimoto, J. A. Izatt, and V. V. Tuchin, Eds., vol. 7889, SPIE, p. 78890Z.

[15] SUN, D., ROTH, S., AND BLACK, M. J. Secrets of optical flow estimation and their principles. In *CVPR'10* (2010), pp. 2432–2439.

[16] WANG, W., ISHIJIMA, R., MATSUDA, A., HANSON, S. G., AND TAKEDA, M. Pseudo-stokes vector correlation from complex signal representation of a speckle pattern and its applications to micro-displacement measurement. *Strain 46* (2010), 12–18.